Chinese Chemical Letters 36 (2025) 109967

Contents lists available at ScienceDirect

Chinese Chemical Letters

journal homepage: www.elsevier.com/locate/cclet

Highly selective [4+4] cross-photodimerization of (4a-azonia)anthracenes driven by confinement of D-A hetero-guest pair in cucurbit[10]uril host

Xianchen Hu[a], Junli Yang[a], Fang Gao[a], Zhiyong Zhao[a,b], Simin Liu[a,b,*]

[a] School of Chemistry and Chemical Engineering, Wuhan University of Science and Technology, Wuhan 430081, China
[b] The State Key Laboratory of Refractories and Metallurgy, Institute of Advanced Materials and Nanotechnology, Wuhan University of Science and Technology, Wuhan 430081, China

ARTICLE INFO

Article history:
Received 23 February 2024
Revised 19 April 2024
Accepted 5 May 2024
Available online 6 May 2024

Keywords:
Supramolecular catalysis
Cross-photodimerization
Host-guest complexation
Charge-transfer interaction
Cucurbit[10]uril

ABSTRACT

The cross-photodimerization often comes with the formation of undesired and competitive homo-photodimer as side products. Herein, we report a series of highly selective [4 + 4] cross-photodimerization between anthracene and 4a-azoniaanthracene derivatives within a cucurbit[10]uril (CB[10]) host in water. Heteroternary inclusion complexes were formed through encapsulation of donor (**D1**-**D2**, anthracene derivative) and acceptor (**A1-A3**, 4a-azoniaanthracene derivatives) pairs in CB[10]. In the presence of CB[10] (1.0 equiv.), the [4 + 4] cross-photodimerization between **D1** and **A1**/**A2**/**A3** efficiently gave a single racemic cross-photodimer. Furthermore, the cross-photodimerization between 9-substituted anthracene **D2** and **A1**/**A3** was catalyzed by CB[10] (0.1 equiv.) to quantitatively yield a cross-photodimer with high regioselectivity. Efficient formation of selective cross-photodimers could be attributed to the exclusive encapsulation of D-A hetero-guest pairs in CB[10] and the confinement effect of the CB[10] host cavity. Our study further proves host–guest complexation as a powerful strategy for cross-cycloaddition reactions with high efficiency.

Photochemical reactions involving anthracene and its derivatives, including photodimerization and other reactions, have been widely investigated over the past 100 years [1]. Furthermore, anthracene dimerization has been further used in the design of chiral ligand, carbon nanoring, molecular cage switch and optical materials/devices [2-4]. However, due to the poor reaction selectivity and homo-photodimerization as side reaction, till now only few intermolecular [4 + 4] cross-photodimerizations between anthracene and its derivatives have been reported [5-7]. Inspired by the natural features of enzymes, supramolecular nanoreactors/catalysts with confined cavities, often referred to as artificial enzymes, have been developed and made significant advancements in various types of organic reactions [8-14]. Supramolecular host working as nanoreactors/catalysts can profoundly govern reactivity and selectivity [15-17]. By introducing a host–guest complexation strategy, researchers have achieved enhanced efficiency and even stereoselectivity in the homo-photodimerization of anthracene derivatives [18]. However, to date, there is no efficient way to improve the cross-photodimerization between anthracene derivatives.

Cucurbit[*n*]uril (CB[*n*], $n = 5$–8, 10), a family of molecular containers known for their high binding affinity and selectivity toward cationic and neutral guests [19,20], have also been employed to promote various organic reactions [8,21-23]. CB[10] (Fig. 1A), which has the largest cavity among CB[*n*], has shown its remarkable capacity to accommodate large-sized molecules or donor-acceptor guest pair to form heteroternary complex by host-stabilized charge-transfer (HSCT) interaction (charge transfer interaction between a pyridinium and an aromatic ring is also defined as cation–π interaction [17]) [24-27]. Building upon our previous research involving CB[10]-catalyzed homo-photodimerization of anthracene or azaanthracene derivatives [28,29], we started to investigate the cross-photodimerization between anthracene and 4a-azoniaanthracene derivatives. We envisioned that by combining the selective encapsulation of the D-A pair with the pre-orientation of guests within CB[10], the intermolecular [4 + 4] cross-photodimerization between anthracene and 4a-azoniaanthracene derivatives could be accomplished with high efficiency (Fig. 1B).

* Corresponding author.
E-mail address: liusimin@wust.edu.cn (S. Liu).

https://doi.org/10.1016/j.cclet.2024.109967
1001-8417/

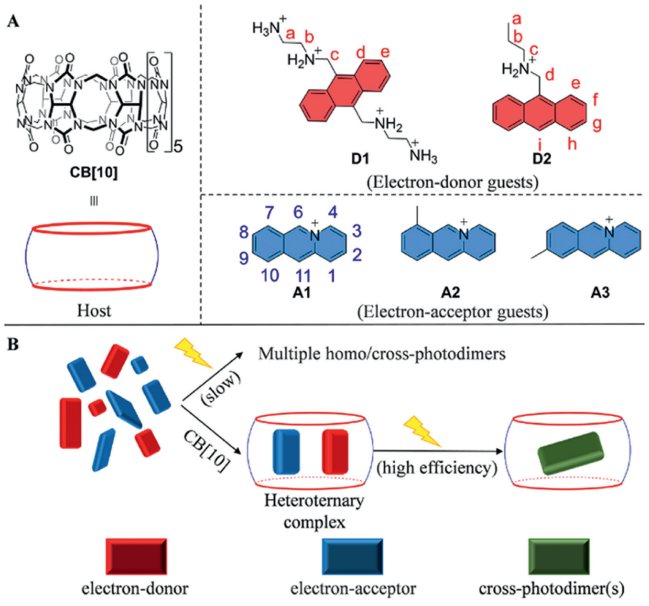

Fig. 1. (A) Chemical structures of CB[10], electron-donor guests (**D1**-**D2**) (counterions are Cl^-), and electron-acceptor guests (**A1**-**A3**) (counterions are Br^-) (all anions were omitted for clarity). (B) Schematic illustration of host–guest complexation strategy for cross-photodimerization of D-A pair.

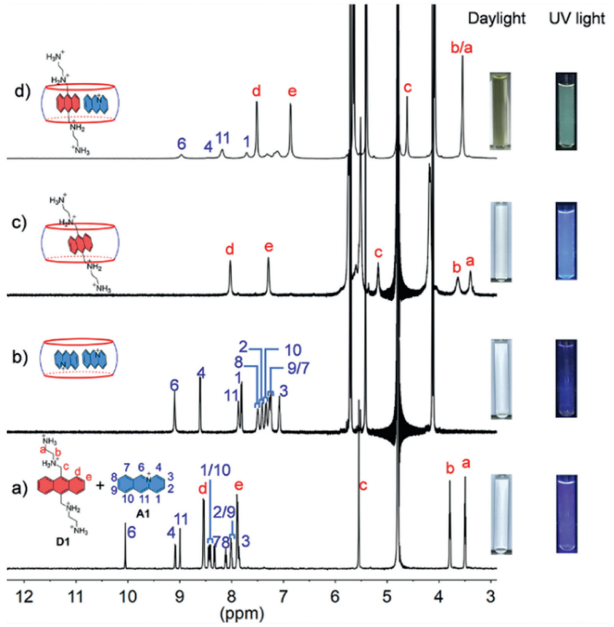

Fig. 2. ^{1}H NMR spectra (600 MHz, D_2O, 298 K) of (a) an equimolar mixture of **D1** and **A1** ([**D1**] = [**A1**] = 2.5 mmol/L). (b) **A1** with 0.5 equiv. of CB[10], (c) **D1** with 1.0 equiv. of CB[10], (d) an equimolar mixture of **D1** and **A1** with 1.0 equiv. of CB[10]. Photographs of samples in NMR tubes were taken under natural light and photoexcitation at 365 nm.

The synthesis and characterization of donor molecules **D1**-**D2** and acceptor molecules **A1**-**A3** (Fig. 1A) were presented in the supplemental information (Scheme S1 and Figs. S1-S7 in Supporting information). In order to analyze the products after photoirradiation of D-A pairs, the homo-photodimerization reaction of each compound was investigated firstly. **D1** did not undergo homo-photodimerization and the photoirradiation of **D2** for 12 h afforded head-to-tail (HT) dimer HT-$P_{\mathbf{D2}\text{-}\mathbf{D2}}$ (structural identification of HT-$P_{\mathbf{D2}\text{-}\mathbf{D2}}$ was based on our previous report [28]) (Fig. S8 in Supporting information). **A1** underwent homo-photodimerization to afford four regioisomeric photodimers (*anti*-HT, *syn*-HH, *rac-anti*-HH, *rac-syn*-HT) identified by ^{1}H NMR spectra (Fig. S9 in Supporting information) [30-32]. Similar to **A1**, **A2**-**A3** produced four regioisomeric photodimers upon photoirradiation (Figs. S10 and S11 in Supporting information). We also investigated the complexation of each guest with CB[10]. ^{1}H NMR titration experiments revealed that the signals for the aromatic protons of **D2** and **A1**-**A3** underwent significant upfield shifts, suggesting that anthracene or 4a-azoniaanthracene units on guests were encapsulated by CB[10] to form inclusion complexes. ESI-MS analysis further confirmed that all guests (**D2** and **A1**-**A3**) formed 1:2 host–guest homoternary complexes with CB[10] (Fig. S12-S19 in Supporting information).

The host–guest complexation between the hetero-guest pair **D1**-**A1** and CB[10] was investigated by ^{1}H NMR, fluorescence, and ESI-MS spectroscopies. ^{1}H NMR spectra analysis showed that all proton signals of **D1** and **A1** in their equimolar mixture in the absence of CB[10] remained unchanged, implying no obvious interaction between **D1** and **A1** (Fig. 2a). However, the observation of shifted proton signals of **D1** and **A1** in the presence of CB[10] compared to CB[10]·**D1** and CB[10]·$\mathbf{A1}_2$ confirmed the formation of the heteroternary inclusion complex CB[10]·**D1**·**A1** (Figs. 2b-d). Since the binding between CB[10] and **D1** displayed slow exchange kinetics on the ^{1}H NMR time scale [28], and no proton signals of **D1** in CB[10]·**D1** were found in the ^{1}H NMR spectra of the mixture of **D1**, **A1**, and CB[10] (compare Fig. 2c with Fig. 2d), it was highly likely that CB[10]·**D1**·**A1** exclusively formed. Multiple cross peaks in a ROESY spectrum of the hetero-guest pair and CB[10] mixture suggested that **D1** and **A1** were in close proximity (Fig. S20 in Supporting information). Additionally, the transparent solution of an equimolar mixture of **D1** and **A1**, with a blue emission at 408 nm, turned yellow and displayed a red-shifted emission at 517 nm (yellow-green fluorescence) upon adding 1.0 equiv. of CB[10] (Fig. S21 in Supporting information). This change indicated the weak CT interaction between electron-rich guest **D1** and electron-deficient guest **A1** was significantly enhanced by the presence of CB[10] [27,33]. ESI-MS also confirmed the exclusive existence of the heteroternary inclusion complex CB[10]·**D1**·**A1** (Fig. S22 in Supporting information): the ion peak at *m/z* 721.604 corresponded to the 1:1:1 complex CB[10]·**D1**·**A1** ([CB[10] + **D1** + **A1** – $2H^+$]$^{3+}$ = 721.601). The exclusive formation of the heteroternary complex CB[10]·**D1**·**A1** implied the possibility of efficient cross-photodimerization of **D1**-**A1** pair within the host.

Fig. 3A and Fig. S23A (Supporting information) presented a schematic of CB[10]-mediated intermolecular cross-photodimerization between **D1** and **A1**. As depicted in Fig. S23B(b), after UV irradiation for 3 h, the ^{1}H NMR spectrum of **D1** and **A1** showed complicated new peaks representing photoproducts, with much unreacted **D1** and **A1** remaining in the solution. Further analysis disclosed that only 41% of **A1** was converted into four regioisomeric homo-photodimers (*anti*-HT-$P_{\mathbf{A1}\text{-}\mathbf{A1}}$, *syn*-HH-$P_{\mathbf{A1}\text{-}\mathbf{A1}}$, *rac-anti*-HH-$P_{\mathbf{A1}\text{-}\mathbf{A1}}$, *rac-syn*-HT-$P_{\mathbf{A1}\text{-}\mathbf{A1}}$; 36% relative yield). These products were identified by comparing Fig. S23B(b) to Fig. S9. Additionally, there was a cross-photodimer, *rac*-$P_{\mathbf{D1}\text{-}\mathbf{A1}}$, formed in 64% relative yield. In contrast, in the presence of 1.0 equiv. of CB[10], the proton signals of bound **D1** and **A1** gradually diminished and completely disappeared after 50 min, with the appearance of new peaks representing photoproduct(s) (Figs. S23B(c) and (d), Fig. S24 in Supporting information). The photoproduct was identified as the pure cross-photodimer *rac*-$P_{\mathbf{D1}\text{-}\mathbf{A1}}$ in nearly quantitative yield (characterization data for *rac*-$P_{\mathbf{D1}\text{-}\mathbf{A1}}$ were showed in Figs. S25-S27 in Supporting information). Notably, the sample of *rac*-$P_{\mathbf{D1}\text{-}\mathbf{A1}}$ used for ^{1}H NMR (Fig. S23B (e)) was obtained by competitive guest displacement without further purification. This indicated the exclusive hetero-pairwise selectivity of CB[10] and highly efficient cross-photodimerization between **D1** and **A1**

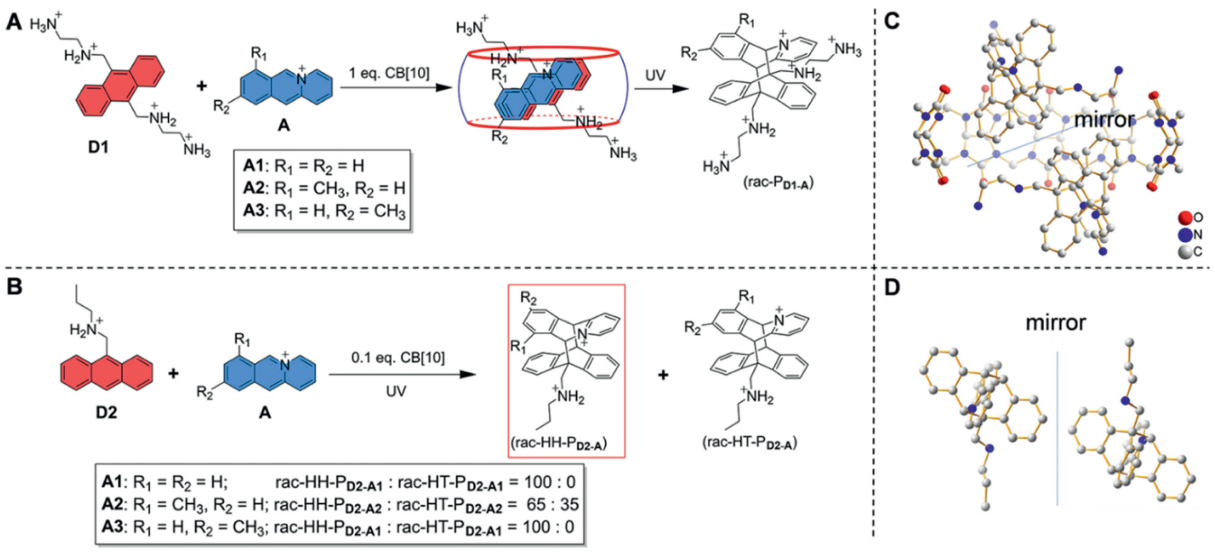

Fig. 3. Schematic illustration of CB[10]-mediated intermolecular [4 + 4] cross-photodimerization between **D1**/**D2** and **A1**/**A2**/**A3** (A, B). X-ray crystal structures of the host-product inclusion complex CB[10]·(±)$P_{\mathbf{D1\text{-}A1}}$ (cutaway view of CB[10]) (C) and (±)HH-$P_{\mathbf{D2\text{-}A1}}$ (D). Hydrogen atoms, solvent molecules and anions were omitted for clarity.

within CB[10]. Given that "the intra-complex photodimerization is unimolecular in nature" [34], an apparent rate constant (k_1) of the cross-photodimerization reaction between **D1** and **A1** with 1.0 equiv. of CB[10] was calculated to be 0.04044 ± 0.00253 min^{-1} using pseudo-first-order kinetics (Fig. S28 in Supporting information). Clearly, all of these data proved that CB[10] functioned as a supramolecular nanoreactor in this case to accelerate the cross-photodimerization reaction and improve the reaction selectivity (avoiding homo-photodimerization).

Single crystals of the inclusion complex CB[10]·(±)$P_{\mathbf{D1\text{-}A1}}$ were obtained through the slow evaporation of an irradiated aqueous solution containing **D1**, **A1**, and CB[10], confirming the structure of the cross-photodimer *rac*-$P_{\mathbf{D1\text{-}A1}}$ (Fig. 3C). Surprisingly, a pair of racemic enantiomers, (±)$P_{\mathbf{D1\text{-}A1}}$, were co-encapsulated by a single CB[10] molecule to form a 1:2 racemic inclusion complex CB[10]·(±)$P_{\mathbf{D1\text{-}A1}}$. This differed from the observation of the co-existence of homo-chiral and hetero-chiral CB[10]-based ternary inclusion complexes [35]. Moreover, the 1:2 binding mode in crystal was different from a 1:1 binding mode between CB[10] and $P_{\mathbf{D1\text{-}A1}}$ in aqueous solution (Fig. S29 in Supporting information), which could be attributed to the crystal packing effect [36]. Crystallographic data, including CCDC number, were listed in Table S2 (Supporting information).

The exclusive formation of heteroternary complexes CB[10]·**D1**·**A2** and CB[10]·**D1**·**A3** was aslo verified by NMR, ESI-MS, and fluorence spectroscopies (Figs. S30-S33 in Supporting information). Similar to the cross-photodimerization between **D1** and **A1** in the presence of 1.0 equiv. of CB[10], the photoirradiation of **D1** and **A2**/**A3** exclusively yielded *rac*-$P_{\mathbf{D1\text{-}A2}}$/*rac*-$P_{\mathbf{D1\text{-}A3}}$ (Fig. 3A, Figs. S34-S45 in Supporting information). Single crystals of the inclusion complex CB[10]·(±)$P_{\mathbf{D1\text{-}A3}}$ were also obtained, confirming the structure of the cross-photodimer *rac*-$P_{\mathbf{D1\text{-}A3}}$ (Fig. S46 in Supporting information). In comparison, although having an extra methyl substituent at a different position, **A2**/**A3** reacted with **D1** similarly to **A1** in the presence of CB[10]. Detailed cross-photodimerization data were provided in Table S1 (Supporting information).

The characterization of the heteroternary inclusion complex CB[10]·**D2**·**A1** was illustrated in Fig. S47 (Supporting information). The typical chemical shift changes upon the addition of CB[10], the emission color change from blue (the solution of **D2**-**A1**) to vibrant yellow (the solution of **D2**-**A1** with CB[10]), and ESI-MS confirmed the encapsulation of the **D2**-**A1** pair in CB[10]. In a similar manner, we investigated the host–guest complexations of **D2** and **A2**/**A3** with CB[10] (Figs. S49-S52 in Supporting information). All of data verified that the **D2**-**A** pairs could be encapsulated by CB[10].

The cross-photodimerization between **D2** and **A1** with CB[10] was shown in Fig. 3B. Photoirradiation of the mixture of **D2** and **A1** for 6 h afforded seven photoproducts: the homo-photodimer HT-$P_{\mathbf{D2\text{-}D2}}$ in a relative yield of 31%, four homo-photodimers from **A1** in 27%, the cross-photodimer *rac*-HH-$P_{\mathbf{D2\text{-}A1}}$ in 29%, and *rac*-HT-$P_{\mathbf{D2\text{-}A1}}$ in 13%, with a total conversion of 76% (Fig. S53, Table S1 in Supporting information). Relatively, in the presence of 0.1 equiv. of CB[10], the proton signals of **D2** and **A1** gradually disappeared under UV irradiation and eventually vanished after 2 h, with appearance of new and sharp proton signals representing the product(s) (Fig. S54 in Supporting information). After work-up, the photoproduct was identified to be the pure cross-photodimer *rac*-HH-$P_{\mathbf{D2\text{-}A1}}$ (Figs. S55-S57 in Supporting information). Single crystals of *rac*-HH-$P_{\mathbf{D2\text{-}A1}}$ unambiguously confirmed its HH configuration (Fig. 3D). An apparent rate constant (k_1) for the cross-photodimerization of the **D2** and **A1** pair with 0.1 equiv. of CB[10] was then calculated to be 0.02852 ± 0.00093 min^{-1} with pseudo-first-order kinetics (Fig. S58a in Supporting information). To gain insight into why CB[10] can catalyze this cross-photodimerization reaction with high regioselectivity, we performed density functional theory (DFT) calculations. As depicted in Fig. 4, the energy of the heteroternay complex HH–CB[10]·**D2**·**A1** was significant lower, by 84.1 kcal/mol, than that of HT-CB[10]·**D2**·**A1**, accounting for the exclusive formation of the cross-photodimer *rac*-HH-$P_{\mathbf{D2\text{-}A1}}$. The energy of CB[10]·*rac*-HH-$P_{\mathbf{D2\text{-}A1}}$ was 31.8 kcal/mol higher than that of HH–CB[10]·**D2**·**A1**, resulting in the occurrence of the catalytic cycle. Therefore, the cross-photodimerization between **D2** and **A1** catalyzed by CB[10] with high conversion and regio-selectivity, could be illustrated as in Fig. S58b (Supporting information).

Unexpectedly, while CB[10] could still catalyze the cross-photodimerization reaction between **D2** and **A2**, two regioisomeric cross-photodimers *rac*-HH-$P_{\mathbf{D2\text{-}A2}}$ and *rac*-HT-$P_{\mathbf{D2\text{-}A2}}$ were obtained with relative yields of 65% and 35%, respectively (Figs. S59-S63, Table S1 in Supporting information). We speculated that the introduction of a 7-substituted methyl group on **A2** led to the formation of both HH and HT arrangements, even though the heteroternary complex CB[10]·**D2**·**A2** exclusively formed. Indeed, DFT calculations suggested that the energies of HH–CB[10]·**D2**·**A2** and HT-CB[10]·**D2**·**A2** were almost identical (Table S3 in Supporting in-

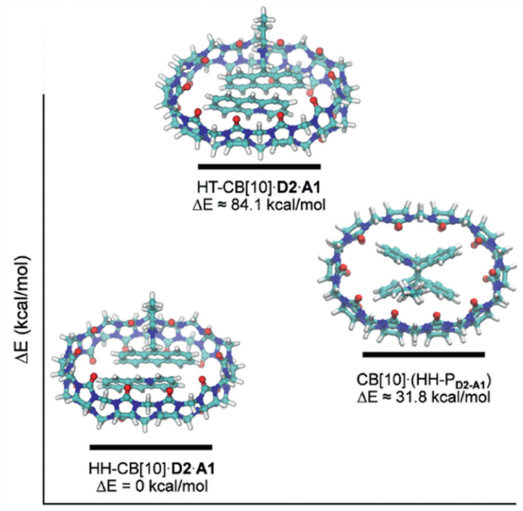

Fig. 4. Energy-optimized structures of heteroternary complex HH/HT-CB[10]·**D2**·**A1** and host-photodimer complex CB[10]·HH-P$_{\mathbf{D2\text{-}A1}}$ (B3LYP-D3/6–31G* level of theory). The lowest energy of the heteroternary complex HH–CB[10]·**D2**·**A1** was set at 0 kcal/mol. C, cyan; N, blue; O, red; H, white.

formation), explaining the low regioselectivity in this case. The cross-photodimerization between **D2** and **A3** was catalyzed by CB[10] to give a single cross-photodimer *rac*-HH-P$_{\mathbf{D2\text{-}A3}}$ (Figs. S64-S69 and Table S1 in Supporting information).

In summary, we have illustrated unreported examples of [4 + 4] cross-photodimerizations between anthracene and 4a-azoniaanthracene derivatives mediated by a host molecule. The CB[10] host demonstrated its remarkable ability to selectively encapsulate pairs of electron-donor (D) and electron-acceptor (A) molecules and significantly enhance the charge-transfer interaction between D and A molecules. The use of CB[10] as a host provided cross-photodimerization reactions between anthracene and 4a-azoniaanthracene derivatives with high reaction rate, yield, and selectivity. In the best example, only one single regioisomer as a cross-photodimer was yielded in the presence of a catalytic amount of CB[10]. This improvement can be attributed to the exclusive hetero-pairwise selectivity and nanoconfinement effect of CB[10]. These findings not only contribute to the understanding of supramolecular host–guest chemistry but also offer practical applications in the field of organic synthesis, particularly in cross-photocycloaddition reactions. Our work further paves the way for the exploration of supramolecular hosts and their potential in controlling and enhancing various chemical reactions. Given the significance of heteroternary complexes in the design of light-controlled supramolecular machines or fluorescence switches [37], we anticipate that our system could also make valuable contributions in this area.

Declaration of competing interest

The authors declare that they have no known competing financial interests or personal relationships that could have appeared to influence the work reported in this paper.

CRediT authorship contribution statement

Xianchen Hu: Writing – review & editing, Writing – original draft, Data curation, Conceptualization. **Junli Yang:** Writing – review & editing. **Fang Gao:** Writing – review & editing. **Zhiyong Zhao:** Writing – review & editing. **Simin Liu:** Writing – review & editing, Project administration, Conceptualization.

Acknowledgments

This work was financially supported by the National Natural Science Foundation of China (No. 21871216). DFT calculations were supported by High-Performance Computing Center at Wuhan University of Science and Technology.

Supplementary materials

Supplementary material associated with this article can be found, in the online version, at doi:10.1016/j.cclet.2024.109967.

References

[1] W. Liu, L. Guo, Y. Fan, et al., Chin. J. Org. Chem. 37 (2017) 543–554.
[2] X. Wang, W.G. Liu, L.T. Liu, et al., Org. Lett. 23 (2021) 5485–5490.
[3] W. Xu, X.D. Yang, X.B. Fan, et al., Angew. Chem. Int. Ed. 58 (2019) 3943–3947.
[4] W. Zhou, Y. Chen, Q. Yu, et al., Chem. Sci. 10 (2019) 3346–3352.
[5] H. Bouas-Laurent, A. Castellan, J.P. Desvergne, Pure Appl. Chem. 52 (1980) 2633–2648.
[6] Y. Kawanami, H. Umehara, J.I. Mizoguchi, et al., J. Org. Chem. 78 (2013) 3073–3085.
[7] D. Bailey, N. Seifi, V.E. Williams, Dyes Pigments 89 (2011) 313–318.
[8] L. Wang, C. Su, Supramolecular Catalysts, World Scientific, Singapore, 2020.
[9] D.S. Dalal, D.R. Patil, Y.A. Tayade, Chem. Rec. 18 (2018) 1560–1582.
[10] P. Neri, J.L. Sessler, M.X. Wang, In Calixarenes and Beyond, Springer, 2016.
[11] Y. Xue, X. Hang, J. Ding, et al., Coord. Chem. Rev. 430 (2021) 213656.
[12] C. Wang, L. Xu, Z. Jia, et al., Chin. Chem. Lett. 35 (2024) 109075.
[13] M. Yoshizawa, M. Tamura, M. Fujita, Science 312 (2006) 251–254.
[14] J.S. Wang, K. Wu, C. Yin, et al., Nat. Commun. 11 (2020) 4675.
[15] Y. Jiao, X.Y. Chen, J.F. Stoddart, Chem 8 (2022) 414–438.
[16] K. Wang, J.H. Jordan, X.Y. Hu, et al., Angew. Chem. Int. Ed. 59 (2020) 13712–13721.
[17] S. Yamada, Chem. Rev. 118 (2018) 11353–11432.
[18] M. Rao, W. Wu, C. Yang, Green Synth. Catal. 2 (2021) 131–144.
[19] S.J. Barrow, S. Kasera, M.J. Rowland, et al., Chem. Rev. 115 (2015) 12320–12406.
[20] X.L. Ni, X. Xiao, H. Cong, et al., Acc. Chem. Res. 47 (2014) 1386–1395.
[21] K.I. Assaf, W.M. Nau, Chem. Soc. Rev. 44 (2015) 394–418.
[22] B. Tang, J. Zhao, J.F. Xu, et al., Chem. Eur. J. 26 (2020) 15446–15460.
[23] H. Barbero, E. Masson, In: K. Kim (Ed.), Cucurbiturils as reaction vessels, Cucurbiturils and Related Macrocycles, Royal Society of Chemistry, 2019, pp. 86–120.
[24] X. Yang, F. Liu, Z. Zhao, et al., Chin. Chem. Lett. 29 (2018) 1560–1566.
[25] Y.L. Lu, X.D. Zhang, Y.H. Qin, et al., Chem 9 (2023) 2144–2160.
[26] W. Gong, X. Yang, P.Y. Zavalij, et al., Chem. Eur. J. 22 (2016) 17612–17618.
[27] J. Yang, X. Hu, M. Fan, et al., Org. Chem. Front. 10 (2023) 422–429.
[28] X. Hu, F. Liu, X. Zhang, et al., Chem. Sci. 11 (2020) 4779–4785.
[29] H. Li, X. Hu, F. Liu, et al., Chin. Chem. Lett. 33 (2022) 5124–5127.
[30] S.A. Stratford, M. Arhangelskis, D.K. Bučar, et al., CrystEngComm 16 (2014) 10830–10836.
[31] H. Ihmels, J. Luo, J. Photochem. Photobiol. A: Chem. 200 (2008) 3–9.
[32] T. Wolff, C. Lehnberger, D. Scheller, Heterocycles 45 (1997) 2033–2039.
[33] D. Sun, Y. Wu, X. Han, et al., Nat. Commun. 14 (2023) 4190.
[34] X. Wei, W. Wu, R. Matsushita, et al., J. Am. Chem. Soc. 140 (2018) 3959–3974.
[35] S. Liu, P.Y. Zavalij, L. Isaacs, J. Am. Chem. Soc. 127 (2005) 16798–16799.
[36] N. Hickey, B. Medagli, A. Pedrini, et al., Cryst. Growth Des. 21 (2021) 3650–3655.
[37] J. Gemen, J.R. Church, T.P. Ruoko, et al., Science 381 (2023) 1357–1363.